https://doi.org/10.5194/egusphere-2026-2374
Preprint. Discussion started: 20 May 2026

Comparing AERONET integrated water vapor with GNSS over the Arctic in the context of former comparisons with radiosondes and reanalyses.

Victoria E. Cachorro[1,2], Juan Carlos Antuña-Marrero[3,1], Abel Calle[1,2], Roberto Román[1,2], David Mateos[1,2], Carlos Toledano[1,2], Juan Carlos Antuña-Sánchez[4, 1], Ramiro González[1,2], Manuel Antón[5,6], Javier Vaquero-Martínez[7,6], Ángel M. de Frutos Baraja[1,2] and Javier Pacheco[1]

[1]Group of Atmospheric Optics (GOA-UVa), Universidad de Valladolid, 47011, Valladolid, Spain
[2]Laboratory of Disruptive Interdisciplinary Science (LADIS), Universidad de Valladolid, Valladolid 47011, Spain
[3]Instituto de Geociencias (IGEO), Consejo Superior de Investigaciones Científicas (CSIC) - Universidad Complutense de Madrid (UCM), Madrid 28040, Spain
[4]GRASP-SAS, Villeneuve d'Ascq, France
[5]Department of Physics, Universidad de Extremadura, 06006 Badajoz, Spain
[6]Instituto Universitario de Investigación del Agua, Cambio Climático y Sostenibilidad (IACYS), Universidad de Extremadura, 06006 Badajoz, Spain
[7]Departamento de Didáctica de las Ciencias Experimentales y las Matemáticas, Universidad de Extremadura, 10071 Cáceres, Spain

Correspondence to: Juan Carlos Antuña-Marrero (jcam45@gmail.com)

Abstract. The Integrated Water Vapor (IWV) determination in the Arctic is very important for atmospheric-climate studies. Different measurements and techniques are used for this purpose, having in general low spatial and temporal resolutions, except the Global Navigation Satellite Systems (GNSS), especially in the Arctic due to extreme weather conditions. In this work, the comparison of IWV measured by sun photometers (SP) from AERONET (IWVSP) and IWV measured by GNSS (IWVGNSS) at Arctic sites, is carried out. Taking coincident hourly averaged data IWVSP from 13 AERONET and 35 IWVGNSS sites were selected, covering the period 1997 to 2023. The comparison IWVGNSS versus IWVSP presents very good statistic indicators with the range of absolute and relative Mean Bias Error MBE (rMBE) of 0.007(0.8%)-0.091(15.4%) cm and standard deviation STD (rSTD) of 0.047(6.5%)-0.123(14.4%) cm. The positive bias at all sites detects a dry bias of SP respect to GNSS. Linear regression slopes are greater than 1 at nine sites, and lower at four. Those slopes lower than 1 appears related to higher frequency of IWV lower values (very dry conditions). All sites present Pearson correlation coefficients higher than 0.96, showing a low data dispersion. Results show that for IWV low values, less than 1.5 cm, SP predominates over GNSS, and the opposite when IWV values increase. This work complements two previous ones, where IWV from radiosondes and reanalysis were compared with IWVSP. Although the different data-bases, for coincident hourly, the highest values of IWV are given by GNSS, radiosonde, SP and reanalysis in this order.

https://doi.org/10.5194/egusphere-2026-2374
Preprint. Discussion started: 20 May 2026

1 Introduction

Water vapor is the main natural greenhouse gas and the most important absorber in the Earth´s atmosphere, being a key element for the hydrological cycle, vegetation growth, solar radiation, heat terrestrial fluxes, cloud-aerosol formation, and other direct and indirect processes that address the climate system (Trenberth and Stepaniak, 2004; Cubast et al., 2013; Vihma et al., 2016; Douville et al., 2021). Therefore, water vapor is a fundamental atmospheric variable and its measurement is required worldwide for weather prediction and climate change research.

Despite different quantities or parameters are used to define the moisture or its content in the atmosphere: absolute, relative or specific humidity, mixing ratio, density, etc. this work is focused on the Integrated Water Vapor (IWV), also named Precipitable Water Vapor (PWV) quantity. The IWV is defined as assuming a vertical column of air from the ground to the top of the atmosphere with a base of 1 m^2 (or 1 cm^2), the IWV content of this column equals the amount of water if all water vapor was condensed. The commonly used unit is kg/m^2, reflecting the weight of the condensed water over 1 m^2 of surface, which is equivalent to 1 mm if water is accumulated on the bottom of the column on normal conditions over the surface of 1 cm^2, then mm (or cm) are also current units.

The IWV can be determined by different instrumental techniques, from classical radiosondes (RS) to radiometric sensors at ground-level, like sun photometers (SP), or satellite platforms using different spectral ranges, from visible to microwave wavelengths. More recently, Global Navigation Satellite Systems (GNSS) technique became a powerful tool for determining IWV due to its higher temporal resolution, rapid site expansion and its demonstrated reliability (Vaquero-Martínez and Antón, 2021). However, RS is still considered today the reference technique for water vapor determination in the scientific community (Miloshevich et al., 2006; Zhang et al., 2019). In addition to these direct IWV measurement methods, IWV from reanalyses data represents a very different methodology, precisely absorbing to a greater or lesser degree these same measurements, and a set of different type of data and models. Certainly, the existence of different set of reanalyses developed by different institutions have steadily improved. Therefore, intercomparison and validation studies between of all these types of data are necessary in the monitoring of water vapor in the atmosphere (Schneider et al., 2010; Weaver et al, 2017; García et al., 2021). Furthermore, the limited spatial and temporal coverage of these measurements in the Arctic restricts their overall representativeness in this region.

Although these inconveniences, the objective of these studies is the characterization and behaviour of IWV in the Arctic analysing the advantages and drawbacks of all these different types of data. In Rinke et al. (2019) a deep study was carried out over the Arctic where positive trends of IWV are analysed using reanalyses (IWV_{Rean}) and radiosonde (IWV_{RS}) data over a long period of 30 years (1979-2016). Increases in IWV is found over the central and sub-Arctic based on multiple reanalyses with some corroboration from sparse in situ data, although some differences are found due to the extended analysed area (Vihma et al., 2016; Rinke et al., 2019; Nygård et al., 2020). Powerful amplifying feedbacks are associated to increases of the IWV, intensifying the atmospheric moisture transport and heavy precipitation events. Those feedbacks affect the energy

https://doi.org/10.5194/egusphere-2026-2374
Preprint. Discussion started: 20 May 2026

balance between the surface and the atmosphere, causing global changes on global evaporation and precipitation Douville et al., (2021).

The original idea was to study the IWV data from SP (IWV_{SP}) monitoring capacity from the Aerosol Robotic Network (AERONET), Holben et al. (1998), sites in the Arctic. The main reason is that, coupled with the fact that there are not many sites in this vast region, IWV_{SP} data has not been analysed in detail. Therefore, there is no better way than to compare these measurements with other instruments, techniques, or databases, taking into account all available information. Then, our contribution focus on two earlier papers. In the first the IWV_{SP}, belonging to AERONET, was compared with IWV_{RS} in the Arctic (Antuña-Marrero et al., 2022). The second one compared IWV_{SP} with the IWV_{Rean} from the European Centre for Medium-Range Weather Forecasts (ECMWF) fifth Re-Analysis (ERA-5) and from the NASA Global Modelling and Assimilation Office (GMAO) Modern-Era Retrospective Analysis for Research and Applications, Version 2 (MERRA-2) (Antuña-Marrero et al., 2025), respectively. Here, to conclude this comparative work the analysis between spatiotemporal coincident measurements of IWV_{SP} and IWV from GNSS (IWV_{GNSS}) in the Arctic was conducted.

1 Instruments

2.1 Sun photometer

The IWV_{SP} observations from AERONET version 3 level 2.0 daytime products (AERONET, 2025; Giles et al., 2019) from SP located within the Arctic circle are used in this research. The standard SP CIMEL-318 has been the main AERONET instrument operating at the Arctic sites during the periods taken in this study. Details about the CIMEL SP and its methodology for IWV determination can be seen in Antuña-Marrero et al. (2022) and Giles et al. (2019). The advantage of SP is its high precision under cloud free conditions, both for IWV and aerosols. However, its capacity and higher precision to measure IWV has been advertised at a very lower level than its capacity and high precision to measure aerosols. The limitations of SP are its temporal coverage restricted to daylight hours (compared to GNSS capable of taking measurements throughout the day) because its dependence on direct solar radiation restricts measurements to sunny periods. The cloud presence is removed by the cloud screening procedure. However, this limitation can also be seen as an advantage because cloud presence is easily detected and hence reliable removed. According to Smirnov et al. (2004) and Schneider et al. (2010) an estimated IWV_{SP} uncertainty of ±10% can be attributed.

A new SP CIMEL- CE318-T has the capability to cover part of the period at nights, typically conducted between the first and third lunar quarters (moon illumination > 50%), is now been used in many AERONET sites (Barreto et al., 2016). It provides the opportunity to extend the IWV_{SP} and to cover the period of polar night in the Arctic and Antarctic.

2.2 Global Navigation Satellite Systems (GNSS)

Ground-based GNSS stations can retrieve IWV from the zenith total delay (ZTD) that the signal suffers while traveling between the Satellite and the receiver on ground. ZTD is the sum of the zenith hydrostatic delay (ZHD) and zenith wet delay

https://doi.org/10.5194/egusphere-2026-2374
Preprint. Discussion started: 20 May 2026

(ZWD), being the latter due exclusively to water vapor (Bevis et al., 1992). This can be converted into IWV through a multiplication factor that is dependent on the mean temperature of the atmosphere weighted by water vapor profile, known as Davis temperature (Davis et al., 1985). The data is processed by Nevada Geodetic Laboratory (Blewitt et al., 2018). The processing of the GNSS data to produce ZTD values is carried out using Jet Propulsion Laboratory's (JPL) GipsyX 1.0 software, which is fed with JPL's Repro 3.0 orbits and clocks data, and Vienna Mapping Function 1 (Boehm et al., 2006, VMF1) gridded data and mapping function parameters. JPL's data and software can be obtained fromhttps://gipsyx.jpl.nasa.gov/. The Davis temperature is obtained from VMF1 gridded numerical weather model data. All this processing is done by Nevada Geodetic Laboratory, delivering a IWV product in their tropospheric files, together with other variables (ZTD, Davis Temperature, and other variables related with the tropospheric correction in GNSS processing). Currently, the GNSS technique appears as the most feasible to determine the IWV because its good temporal resolution, accuracy and high performance. The high increases of GNSS sites in the last years allows the proper spatial representation of water vapor distribution, which are highly imperative for improving weather predictions accuracy, especially local near real-time prediction. The IWV_{GNSS} uncertainty can be fixed in the range 0.01-0.02 cm (Schneider et al., 2010; Perez-Ramirez et al., 2014; Giles et al, 2019). Schneider et al. (2010) estimate a IWV_{GNSS} precision about 10%, excluding rather dry conditions. Perez-Ramirez et al. (2014) estimated an IWV_{SP} uncertainty of ±5% in agreement with the IWV_{RS} estimated uncertainty reported by Miloshevich et al. (2006). The uncertainty of the calculated of IWV_{SP} (cm) is one sigma, expected to be less than 10% respect to IWV_{GNSS} retrieval (Giles et al. (2019). Following the same procedures in our former comparisons (Antuña-Marrero et al., 2022; 2025), the altitude correction factors (Weaver et al., 2017), considering the differences in altitude between each pair of SP and GNSS sites, were calculated and applied to the IWV_{GNSS} observed values.

3 Methods

3.1 Spatial and temporal coincidence criteria

Likewise, the two cited papers (Antuña-Marrero et al., 2022, 2025), the comparison of the IWV_{GNSS} and IWV_{SP} is carried out on coincident measurements at hourly timescale. The spatial coincidence scale is defined by the GNSS sites in 100 km radii around each SP site. Table 1 contains a detailed information about the 13 SP sites and its corresponding spatial coincident sets of GNSS sites (35 sites in total), including their geographical locations, altitudes and periods of the available measurements. This information is complemented by Fig. 1 showing the geographical distribution of the 13 Arctic SP sites, as in Antuña-Marrero et al., (2025), each of them associated with different GNSS spatially coincident sites. Back to Table 1, the period covered by the available measurements is from 1997 to 2023, been Barrow SP (1997 to 2022) the longest record from both instruments. However, the different sites present very different periods of measurements. The OPAL and PEARL sites are located almost at the same latitude and longitude but they have a little more than half a kilometer altitudes difference, as can be seen in Table 1. They share the same 2 GNSS sites (EUR2 and EURC), however the correction factors applied to the

https://doi.org/10.5194/egusphere-2026-2374
Preprint. Discussion started: 20 May 2026

IWV_{GNSS} measurements by the altitude differences between each GNSS site and each of the corresponding SP sites were different for OPAL and PEARL.

Sun-photometer						GNSS					
Sites	**Lat**	**Long**	**H (m)**	**Begin**	**End**	**Sites**	**Lat**	**Long**	**H (m)**	**Begin**	**End**
Kangerlussuaq	67.0	-50.6	320	2008	2022	KELY	67.0	-50.9	230	1995	2018
						KLSQ	67.0	-50.6	354	2014	2023
Sodankyla	67.4	26.6	184	2007	2023	SOD3	67.4	26.4	301	2013	2023
						SODA	67.4	26.4	300	1996	2023
						SODF	67.4	26.6	203	2017	2018
Andenes	69.3	16.0	379	2002	2022	AND1	69.3	16.1	44	2001	2023
						ANDO	69.3	16.0	414	1999	2011
Ittoqqortoormiit/	70.5	-22.0	68	2010	2021	SCOR	70.5	-21.9	129	2004	2023
ARM_Oliktok_AK	70.5	-149.9	2	2013	2021	DSL1	70.3	-148.5	17	2002	2023
						EDOC	70.3	-148.3	23	2002	2023
						PBOC	70.3	-148.3	20	2002	2015
						PUO1	70.3	-148.3	21	2002	2015
Barrow	71.3	-156.7	8	1997	2022	ATQK	70.5	-157.4	28	2006	2022
						BARO	71.3	-156.7	12	2014	2023
						BASC	71.3	-156.7	13	2011	2015
						BRW1	71.3	-156.8	16	2008	2023
						SG27	71.3	-156.6	9	2002	2023
						UTQI	71.3	-156.6	12	2018	2023
Tiksi	71.6	128.9	17	2010	2015	TIXG	71.6	128.9	47	2010	2023
						TIXI	71.6	128.9	47	1998	2022
						TIXJ	71.6	128.9	47	2005	2010
Resolute_Bay	74.7	-95.0	35	2004	2022	RESC	74.7	-95.0	73	2008	2023
						RESO	74.7	-94.9	20	2000	2023
Thule	76.5	-68.8	225	2007	2023	THGL	76.5	-68.8	36	2017	2023
						THU2	76.5	-68.8	36	1998	2023
						THU3	76.5	-68.8	36	2002	2019
Hornsund	77.0	15.5	12	2004	2023	PPSH	77.0	15.5	52	2020	2023
						WUTH	77.0	15.5	52	2020	2023
Ny_Alesund_AWI	78.9	11.9	7	2017	2022	ESIS	78.1	13.6	46	2020	2023
						NABG	78.9	11.9	43	2019	2022
						NYA1	78.9	11.9	84	1998	2022
						NYA2	78.9	11.9	81	2007	2023
						NYAL	78.9	11.9	79	1994	2022
OPAL	80.0	-85.9	5	2007	2022	EUR2	80.0	-85.9	29	2005	2023
						EURC	80.0	-85.9	38	2008	2023
PEARL	80.1	-86.4	615	2007	2019	EUR2	80.0	-85.9	29	2005	2023
						EURC	80.0	-85.9	38	2008	2023

Table 1 . List of 13 AERONET SP sites with its geographical locations, the altitude H(m) and beginning and ending years of measurements. For each AERONET SP site the coincident GNSS sites in 100 km radius are indicated and the same information is provided.

Our previous comparison of the IWV_{RS} and IWV_{SP} measurements let us make a regional classification of the Arctic in two zones, because the SP instrumental design is linked to the local diurnal cycle of the solar radiation (Antuña-Marrero et al., 2022). Fortunately, the RS measurements are conducted at noon at night during the course of the day; 12 and 00 UTC granting that one of the two IWV_{RS} measurements will match the IWV_{SP} measurements at the local diurnal period, what is clearly seen

https://doi.org/10.5194/egusphere-2026-2374
Preprint. Discussion started: 20 May 2026

in the Fig. 2 of the cited paper. The Greenland and European Arctic (GEA) region includes 7 SP sites (blue stars) while the Russia, Alaska and Canadian Arctic (RACA) includes 6 SP sites (reed diamonds). In this comparison 3 new SP sites were added due to greater availability of GNSS sites compared to the RS sites. Therefore, the areas are no longer the same as in Antuña-Marrero (2022), nor is the total equivalent, but it is yet possible to compare the results of IWV_{GNSS} - IWV_{SP} and IWV_{RS} - IWV_{SP} comparisons.

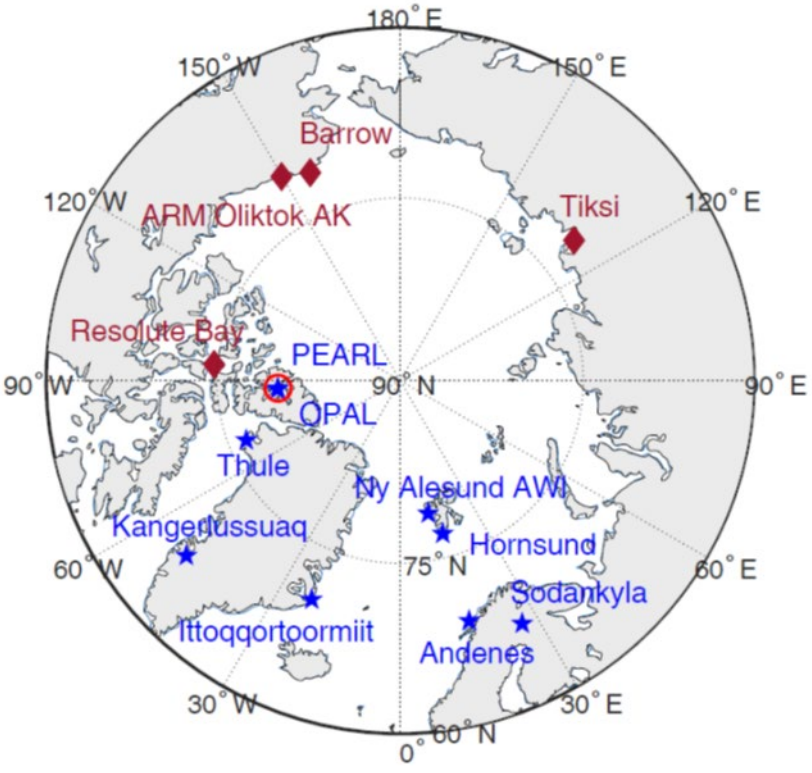

Figure 1. Map of the 13 Arctic AERONET sites used in the present study. Stations in the GEA and RACA regions are identified by blue stars and brown diamonds respectively. The stations names follow the same colors pattern. The very close OPAL and PEARL sites, in north Canada, are identified by a red circle surrounding a blue star.

https://doi.org/10.5194/egusphere-2026-2374
Preprint. Discussion started: 20 May 2026

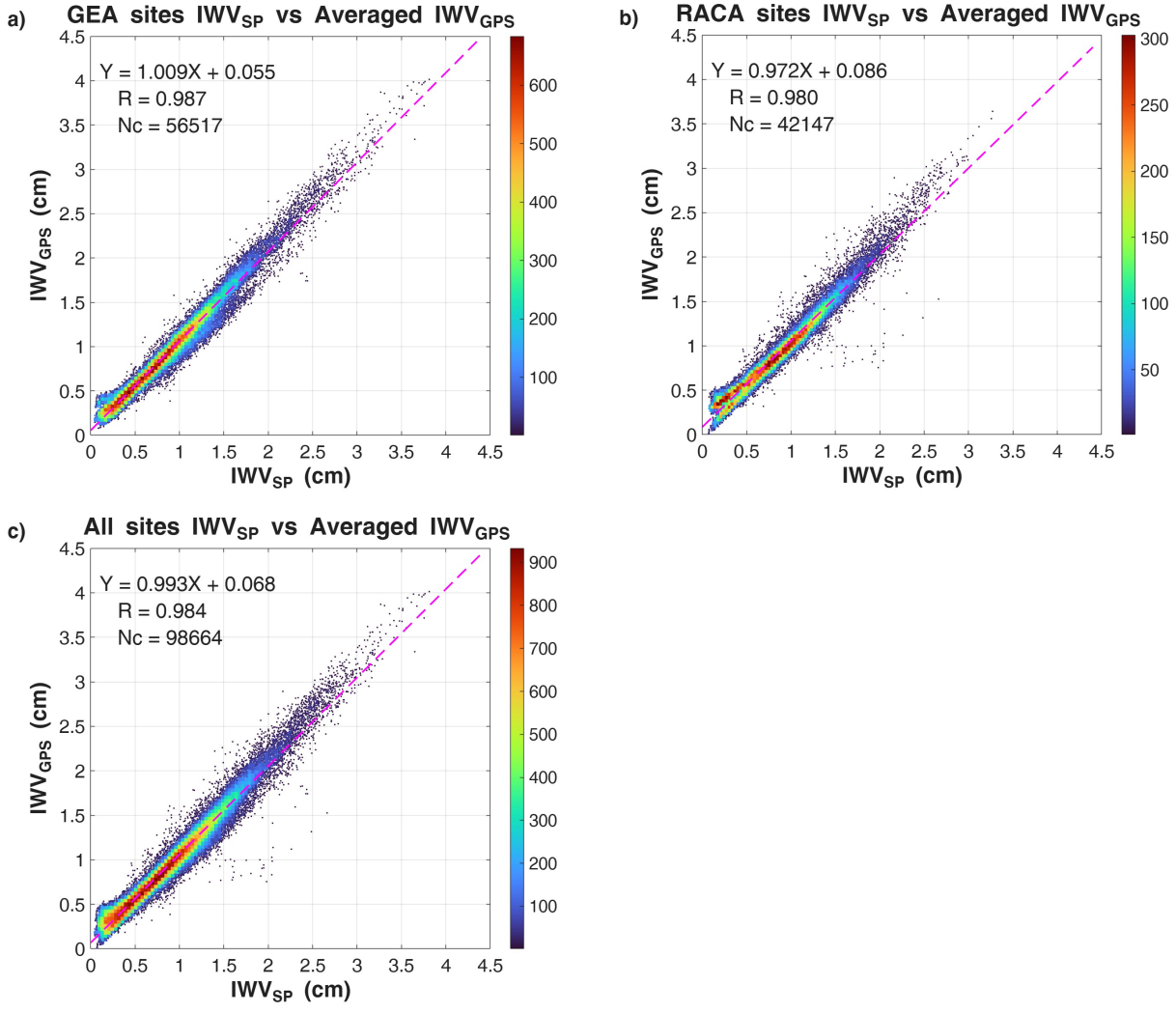

Figure 2 Density scatter plots for time coincident hourly means IWVSP with averaged hourly means IWVGNSS from the coincident GNSS sites in a 100 km radius around each SP site. Nc is the number of coincident measurements. Panel a) sites in GEA region; b) sites RACA region; c) all sites.

3.2 IWV$_{GNSS}$ and IWV$_{SP}$ hourly means

Hourly means, the average of all the instantaneous measurements in the interval of ± 30 minutes around each exact hour, were calculated both for the IWV$_{SP}$ and the altitude corrected IWV$_{GNSS}$ measurements. Then, for each SP site the IWV$_{SP}$ hourly means coincident in time with more than one IWV$_{GNSS}$ hourly means for the coincident GNSS sites were identified and were averaged to produce a unique IWV$_{GNSS}$ hourly value. The resulting set of coincident IWV$_{GNSS}$ and IWV$_{SP}$ hourly mean values were used for the comparison we report here.

https://doi.org/10.5194/egusphere-2026-2374
Preprint. Discussion started: 20 May 2026

3.3 Statistical indicators

Two main statistical indicators were selected for comparing IWV_{GNSS} and IWV_{SP}: the Mean Bias Error (MBE), which defines the mean of the differences $\Delta IWV = (IWV_{GNSS} - IWV_{SP})$ between IWV_{GNSS} and IWV_{SP} and quantifies the accuracy of IWV_{GNSS}, and the standard deviation (STD) of these differences ΔIWV, representing the precision of IWV_{GNSS}. Both statistics are defined in equations (1) and (2), respectively:

$$MBE = \frac{1}{N}\sum_{j=1}^{N}[\Delta IWV_j] \quad (1)$$

$$STD = \sqrt{\frac{1}{N}\sum_{j=1}^{N}[\Delta IWV_j - MBE]^2} \quad (2)$$

where N is the number of pairs of coincident SP and GNSS data. The relative value (in %) of STD (rSTD) and MBE (rMBE) was determined dividing each term by the mean value of IWV_{SP}. In addition, the Pearson linear correlation coefficient (R), the slope (m) and the intercept (yo) of the linear regression fit IWV_{GNSS} versus IWV_{SP} have been calculated

4 Results

4.1 IWV_{GNSS}-IWV_{SP} comparison

Table 2 shows the results of the different statistic indicators of the comparative study between the 13 SP sites and the corresponding associated GNSS (35 sites). The absolute and relative Mean Bias Error, MBE (rMBE), varies between the minimum 0.007 cm (0.8%) at Resolute Bay and the maximum of 0.091 cm (15.4%) at PEARL. Closer to this minimum is the site of Kangerlussuaq with 0.014 cm (1.6%). The second site with the highest rMBE=12% is Thule, but it's the sixth in the mist of MBE values, which reflect the low difference in these values between the different sites. The rest of sites move between these ranges of values, but all the values of MBE are low indicating a good accuracy and positives for all the sites giving a dry bias of IWV_{SP} with respect to IWV_{GNSS}.

Site	MBE (cm)	rMBE (%)	STD (cm)	rSTD (%)	Slope	Interc(cm)	R	N
Kangerlussuaq	0.014	1.6	0.123	14.4	0.797	0.187	0.969	9012
Sodankyla	0.075	6.2	0.096	8.0	1.079	-0.020	0.993	6693
Andenes	0.086	8.7	0.068	6.9	1.027	0.059	0.992	9968
Ittoqqortoormiit	0.064	7.8	0.061	7.5	1.102	-0.020	0.993	9093
ARM_Oliktok_AK	0.093	8.8	0.120	11.3	1.049	0.041	0.983	2335
Barrow	0.052	5.3	0.098	10.1	1.066	-0.013	0.989	8371
Tiksi	0.032	2.6	0.097	7.8	1.093	-0.084	0.991	1706
Resolute_Bay	0.007	0.8	0.086	10.0	1.005	0.003	0.979	7363
Thule	0.074	12.0	0.043	7.0	0.985	0.083	0.991	16937
Hornsund	0.069	9.4	0.047	6.5	1.017	0.056	0.994	1450
Ny_Alesund_AWI	0.033	4.5	0.058	7.9	1.050	-0.004	0.994	3364
PEARL	0.091	15.4	0.068	11.5	0.835	0.188	0.986	12141
OPAL	0.076	8.6	0.087	9.8	0.851	0.207	0.981	10231

https://doi.org/10.5194/egusphere-2026-2374
Preprint. Discussion started: 20 May 2026

Table 2 Statistical results of the comparison of the space and time coincident hourly means IWVSP with the average of IWVGNSS hourly means (ΔIWV= (〖IWV〗_GNSS – 〖IWV〗_SP) from individual coincident GNSS sites in a 100 km radius around each SP site.

The absolute and relative standard deviation show a range of 0.047 cm (6.5%) - 0.123 cm (14.4%), having the sites of Hornsund and Kangerlussuaq the respective minimum and maximum values. These values are also low, showing the good agreement between IWV_{GNSS} and IWV_{SP} data. The values for the indicators of the linear fits give high R, with values from 0.97 to 0.99, then showing a low dispersion of data.

The slopes are in the range 0.797 to 1.102 for Kangerlussuaq and Ittoqqortoomiit, with nine sites out of thirteen sites with slopes > 1, where the dry bias of the IWV_{SP} respects the IWV_{GNSS} increases as the IWV value increases. In the rest four sites, Kangerlussuaq, Thule, OPAL and PEARL, the values of the IWV_{SP} dry bias decrease as IWV increases. Analysing in detail these data-fitting by ranges or categories of IWV a possible cause may be a higher frequency of IWV values below 1.5 cm with respect to the other nine sites. These four sites present geographical-physic and meteorological characteristics with respect to the other sites, as higher dry conditions, their proximity to ice layers and a higher latitude (High Arctic). The intercepts range between positive (8 sites) and negative (5 sites) values, from 0.207 to 0.084 cm at OPAL and Tiksi respectively. All these values of the intercept are below the estimated precision, without weight for most of the IWV values.

4.2 IWV GNSS-SP regional and All-Arctic comparison

Table 3 shows the same statistics of the IWV_{GNSS} vs IWV_{SP} comparison in Table 2, but for the two considered regions, RACA and GEA and the total Arctic area. RS and reanalyses comparison with respect to SP will be analysed in the next section, The same values for the MBE=0.062 cm and rMBE=7.5% were obtained for the two areas and hence for the total Arctic area. The values of STD are also very close between them, 0.09 cm, 0.08 cm, and 0.085 cm for each area with relative STD of 11.0%, 9.6%, and 10.2% respectively for RACA, GEA and the entire Arctic. Certainly, the division of these two areas is reasonable due to the time (12 and 00 UTC) of radiosonde measured, the solar cycle and the number values are due to the distribution is more homogeneous between the two areas. This gives rise to more interesting results for discussion analysing the different values for the slopes respect to 1 and positive and negative intercepts for RACA and GEA areas reported in Table 3.

	Region	MBE (cm)	rMBE (%)	STD (cm)	rSTD (%)	Slope	Interc.(cm)	R
GNSS - SP	RACA	0.06	7.5	0.09	11.00	0.97	0.086	0.99
	GEA	0.06	7.5	0.08	9.6	1.01	0.055	0.98
	Arctic	0.06	7.5	0.085	10.2	0.99	0.068	0.98
Sonde – SP (*)	RACA	0.01	1.40	0.09	10.40	0.93	0.04	0.98
	GEA	0.02	2.50	0.09	10.50	0.93	0.00	0.99
	Arctic	0.02	1.90	0.09	10.40	0.93	0.00	0.99
ERA5 - SP	Arctic	0.10	11.60	0.21	24.90	1.12	0.00	0.93
MERRA2 - SP	Arctic	0.15	18.20	0.24	29.50	1.20	-0.02	0.93

Table 3 Regional and all Arctic statistics of the comparisons of IWV measurements from the radiosondes, GNSS, reanalyses ERA5 and MERRA2 with SP measurements. In all the four cases the IWV from the SP was subtracted. (*) Note that the comparative Sonde-SP contains three less sites (see text).

https://doi.org/10.5194/egusphere-2026-2374
Preprint. Discussion started: 20 May 2026

Figure 2 shows the graphs of linear regressions of the IWV_{GNSS} vs IWV_{SP} for the regions RACA and GEA and the total Arctic area. RACA and GEA present slopes of 0.972, and 1.009 respectively, showing that at GEA the dry bias of the IWV_{SP} respects the IWV_{GNSS} increases as the IWV magnitude increases. At RACA the opposite is present, the dry bias of the IWV_{SP} respects the IWVSGNS decreases as the IWV magnitude increases. In the case of the intercepts both are positive with 0,086 cm for RACA and 0.055 cm for GEA.

As it can be seen, each density scatter plot in Fig. 2 shows clearly three zones in the behaviour between GNSS and SP depending on the IWV values: a first zone between 0 cm and 0.5 cm, a second zone of range 0.5-1.7 cm and a third zone above. For low values of IWV, lower that 0.5 cm, IWV_{GNSS} values show a strange shape with high dispersion and high values respect to those of SP. With only these values, always it should obtain a slope higher than 1. However, when the values of IWV increases, both the values of sun photometers and GNSS present a better concordance defining the second zone. More important, taking into account that this zone is that of higher frequency and contains the highest number of data, this zone determines the slope of the whole fit, which may be lower or higher than the prefect 1:1, although it is modulated by the first and third zones. Above 1.7 cm, in the third zone we can observe that whatever the value of the slope, higher or lower than 1, a great dispersion of data points is above the straight line, where IWV_{GNSS} gives higher values than IWV_{SP}. This feature is also observed at the individual sites (not shown). The consideration of the three zones in the linear regression may be different in other regions of the world, far of Arctic area, because the range of IWV values. Also, it must be noted that the boundaries between zones depends on the climatology of the site due to the range of IWV values.

4.3 Collation with other IWV_{GNSS} vs IWV_{SP} comparison

In general, different publications (Schneider et al., 2010; Pérez-Ramirez et al., 2014; Kruczyk, 2015, Campanelly et al, 2018, Vaquero et al., 2022; García et al., 2021) have shown a dependence of the statistical parameters with the values of IWV. In general, higher absolute differences are obtained when the concentration of water vapor increases and the opposite for the relative differences, but this behaviour shows a strong dependence on the IWV range of values (see Fig. 3 of Perez-Ramirez et al., 2014). The dependence of the differences $\Delta IWV = (IWV_{GNSS} - IWV_{SP})$ vs the IWV_{SP} values were analysed by means of the linear regression but not significant dependence was found, with values of 0.063 cm for the slope and -0.006 for the Pearson coefficient R of the regression. This means that the linear regression between the bulk differences and water vapor values is not necessary, a simple look to the figure is enough to observe the tendency. In any case, comparison of binned data between these two variables or directly the comparison of binned data for MBE and STD versus IWV_{SP} data are more illustrative (see Fig. 2 in Vaquero et al., 2022, where MBE and STD increase with IWV_{SP}). To make classes or categories of water vapor ranges (Campanelli et al, 2018) to analyse the behaviour of different statistical indices is an adequate method as we have explained above for the linear regression of IWV_{GNSS} vs IWV_{SP} comparison.

https://doi.org/10.5194/egusphere-2026-2374
Preprint. Discussion started: 20 May 2026

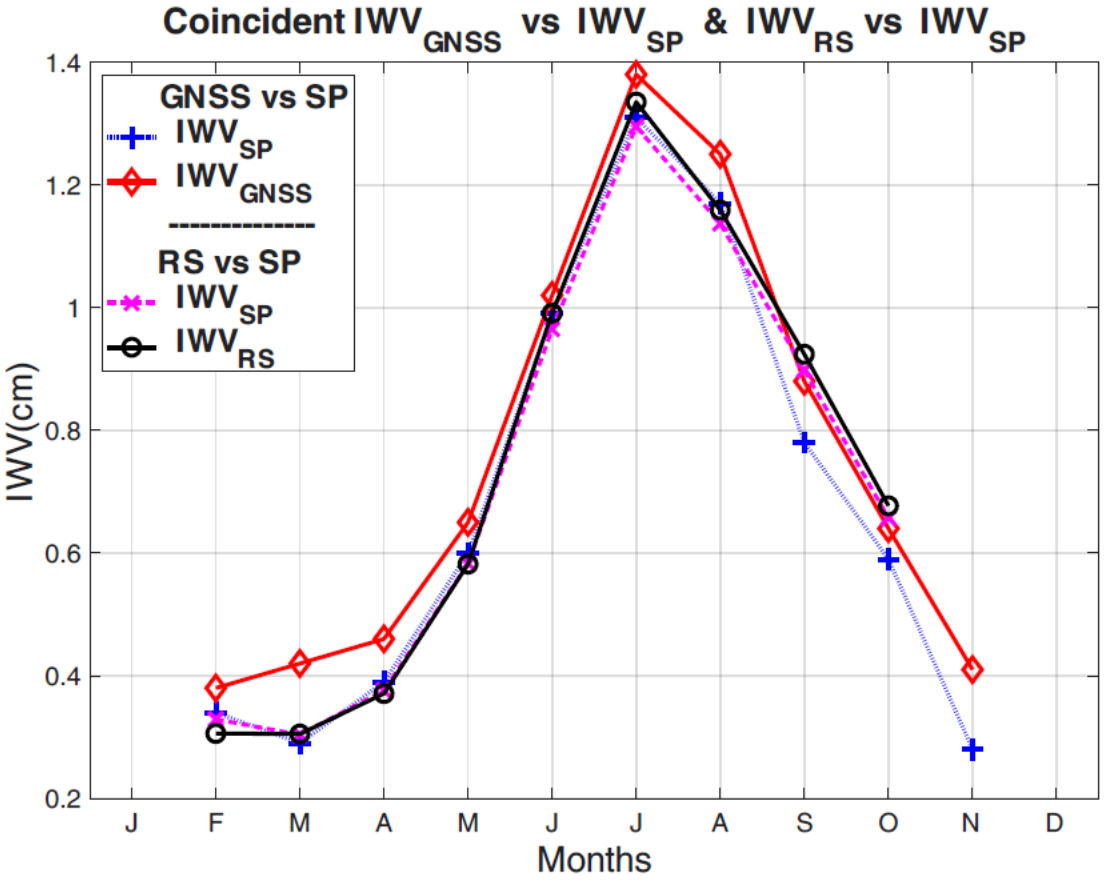

Figure 3 Annual cycles of the coincident values of IWVGNSS and IWVSP used in this comparison. Annual cycles of the coincident values of the IWVRS and IWVSP were calculated with the data used in Antuña-Marrero et al. (2022).

As mentioned, there is no so much analysis in the literature of IWV_{SP} considering the entire wide Arctic area, only a few isolated sites have been studied in several publications (Pérez-Ramirez et al., 2014; Van Malderen et al., 2014, Kruczyk, 2015). Furthermore, there is a big difficulty in the comparison of our results with other publications, basically, by the different database because the time-periods and the criterium of coincidence. However, these limitations, the Barrow site in Pérez-Ramirez et al. (2014), where a clearly dry bias of IWV_{SP} is established in the comparison with IWV_{GNSS}, was compared with values of MBE (rMBE) of 0.06(7.9%) cm and STD (rSTD) 0.07(14.9%) cm, higher than those of Table 2. A slope higher than 1 and a positive intercept of 0.2 mm (Table 2 gives 1 mm but negative) endorses our results at this site. In Van Malderen et al. (2014) three sites: Resolute, Tiksi and Ittoqqortoomiit were monitored in the comparison IWV_{GNSS} vs IWV_{SP} (see Fig. 11), where a positive bias of 0.1 cm is observed for Resolute and negative value about -0.02 for Tiksi and Ittoqqortoomiit, and linear regression slopes of 0.97, 0.94, 0.88 with R2 about 0.98. Kruczyk (2015) provided comparisons for Thule (2009-2014) and Ittoqqortoomiit (2010-2014). Thule has a range of dry SP bias of 0.03-0.12 cm with increasing bias for increasing IWV

https://doi.org/10.5194/egusphere-2026-2374
Preprint. Discussion started: 20 May 2026

values, and STD of 0.054-0.080 cm. Linear regression of slope 1.15 and intercept of -0.06 cm is shown for years 2009-2011. All these supports the IWV_{SP} dry bias. Ittoqqortoomiit (giving values for every year, 2010-2014) presents also a dry SP bias which ranges from a negative value of -0.016 cm (only in 2010) to positive bias that reach the maximum value of 0.025 cm in year 2014 and a STD from 0.049 to 0.071 cm. No linear regression parameters are reported for these or another Arctic sites in this reference.

Not much reliable information from other authors have been obtained in the Arctic area for the IWV_{GNSS} vs IWV_{SP} comparison. Finally, in this work as in the previous ones of Antuña-Marrero et al., (2022, 2025), it was performed the dependence of the differences between IWV_{GNSS} and IWV_{SP} with the solar zenith angle (SZA), which ranges from 45º to 80º, obtaining very low values for the slope, intercept and R, all near zero. Unlike the regression, the differences versus the SZA present a uniform shape mainly due to the short range of angles, indicating the no existence of a clear dependence on the SZA.

4.4 Joint analysis of the comparisons of IWV_{SP} with IWV_{GNSS}, IWV_{RS} and IWV_{Rean}

The comparative analysis of IWV atmospheric variable taking four different techniques, GNSS, radiosondes, reanalysis and sun photometers in the Arctic area highlights the inherent difficulty of comparing our results with those of other authors or publications. Beyond the intrinsic methodological differences of each technique, the difficulty often stems from whether the variables being compared are identical or merely equivalent. By this, we mean the so-called "criterion of spatial and temporal coincidence", which in many cases is not exactly the same, together with the available periods of data, the use of different statistical indicators, and averages when different sites are considered, etc. In addition, the analysis carried out between these three comparatives with SP was based on hourly averages but also the evaluation was made with daily data (not shown) obtaining in general not significant differences, although in general statistical indicators increases (see Antuña-Marrero et al. 2022).

The GNSS and radiosonde techniques have the advantage of being an all-weather conditions methods. However, the difference is that GNSS can work under cloudy and rainy conditions barely affected, and radiosondes can be strongly affected in case of rain. SP or some other radiometric techniques need the presence of the external source as sun, moon or stars, which seem to carry an intrinsic dry bias for removing cloudy conditions. In principle, the algorithms or the methods to apply for removing the effects of rain and clouds are easier in the case of SP that in case of radiosonde. Therefore, a wet affectation of this later is always in mind, and hence the quantification of this uncertainty and its improvement is a real challenging task today.

Following with our primary idea of analysing the capability or performance of SP instruments, in this section a short discussion is carried out about the comparative of IWV_{SP} with IWV_{RS} and IWV_{Rean}. Table 3 shows the results of the statistical indicators for the region of RACA and GEA and the entire Arctic for the three comparisons. However, it must be noted that in the comparative between IWV_{GNSS} vs IWV_{SP} and IWV_{Rean} vs IWV_{SP} three sites were added (Kangerlussuaq, ARM_Olitok_AK, and Thule) to the original IWV_{RS} vs IWV_{SP} comparison using 10 sites (Antuña-Marrero et al., 2022), and also the periods cover of 1997-2023 respect to 1997-2020 for IWV_{RS} are different. In the case of IWV_{Rean} vs IWV_{SP} comparison, no results are

https://doi.org/10.5194/egusphere-2026-2374
Preprint. Discussion started: 20 May 2026

reported for RACA y GEA because a different distribution of sites were made (see Antuña-Marrero, 2025). Although this, the results are indicative enough and the three comparisons highlight the dry bias of SP.

The results IWV_{Rean} vs IWV_{SP} comparison presents the higher values of MBE and STD statistic indicators compared with IWV_{RS} vs IWV_{SP} and IWV_{GNSS} vs IWV_{SP} according to Table 3, with ERA-5 slightly better than MERRA-2. MBE and STD oscillate between 11.6-18.2% and 24.9-29.5%, for ERA-5 and MERRA-2 respectively. Linear least square fitting of IWV_{Rean} vs IWV_{SP} gives slopes around 1.12 for ERA-5 and 1.20 for MERRA-2 and very good values of intercept, practically zero, and relatively good Pearson coefficients, 0.92-0.95. All these numbers emphasize an important dry bias of IWV_{SP} respect to IWV_{Rean}.

The IWV_{RS} vs IWV_{SP} comparison presents a better agreement or lower values of the statistic parameters (Antuña-Marrero et al., 2022 for more detail), thus RS gives high values of IWV than SP for all sites with exception of two sites, Resolute and OPAL. Table 3 shows these lower values for RACA, GEA and entire Arctic: MBE (rMBE) in cm of 0.01(1.4%), 0.02(2.5%), 0.02(1.9%) respectively and the same slopes of 0.93, with practically near zero intercepts.

Therefore, the magnitude of the IWV_{SP} dry bias respect to IWV_{RS}, IWV_{GNSS} and IWV_{Rean} increases in this order. Then the IWV_{SP} values are closer to radiosonde than GNSS. This is demonstrated in the Fig. 3 of the next section, which illustrates the monthly means values for the coincident data of each methodology for the retrieval of IWV. It can be observed as the values of IWV recorded by GNSS are the highest. The finding that the magnitudes of the IWV in both ERA5 and MERRA-2 reanalyses are in general higher than the observations from the three instruments in the Arctic, point to the IWV as another of the variables that may be improved by bias corrections like the cases of tropical temperature and humidity in the context of tropical cyclones from ERA5 (Wei et al., 2025) and global PM2.5 datasets from MERRA-2 (Gupta and Sayeed, 2025). It could be also considered the possibility of the IWV from AERONET sun photometers to be included in the data assimilation or the quality control for the new MERRA-3 and ERA6 reanalyses (El Akkraoui, et al., 2023; Deryng et al., 2024).

In a recent study, Negusini et al. (2021) analysed daily water vapor content with GNSS and radiosonde in the Arctic and Antarctica for about 20 years. Many sites were taken but in the comparison in the Arctic only 9 radiosonde sites were available, four of them are in coincidence with our list. A small dry bias of radiosonde versus GNSS values was found in the Arctic, while no clear behaviour is present in Antarctica. Thus, the results reported by Negusini et al. (2021) confirm our findings in the Arctic.

In the publication of Kruczyk (2015) the comparison of IWV between RS and GNSS was also obtained for 12 sites with a general positive bias for RS (only two sites had a negative value), for a period about three years. These results contradict ours. However, one possible explication is the low values of the bias or the difference between IWV_{RS} and IWV_{GNSS} values and the short period considered, so that our deduction from our comparative RS-GNSS does not allow for such conclusion. It must bear in mind that we did not carry out the direct comparison between IWV values from RS and GNSS.

https://doi.org/10.5194/egusphere-2026-2374
Preprint. Discussion started: 20 May 2026

4.5 IWV_{GNSS}, IWV_{SP} and IWV_{RS} annual cycle

In general, the results of different publications taken data from different sites of the world indicate a dry bias of IWV_{SP} respect to IWV_{GNSS}. This conclusion is based in comparing the coincident data, and averages of different time-scales. For this reason and given the important seasonal variability of IWV in the Arctic, accentuated by the polar night, we have calculated the annual cycle of IWV_{GNSS} and IWV_{SP} reported in Table 4. This is illustrated in Fig. 3 for the whole Arctic area. This figure visualizes more clearly the results of this study. This calculation was performed based on the hourly, daily and monthly averages taking the coincident data of each technique SP and GNSS.

	Coincident SP		Coincident GNSS	
Month	Mean	STD	Mean	STD
J	---	---	---	---
F	0.34	0.13	0.38	0.15
M	0.29	0.14	0.42	0.17
A	0.39	0.15	0.46	0.13
M	0.60	0.20	0.65	0.19
J	0.99	0.24	1.02	0.24
J	1.31	0.30	1.38	0.34
A	1.17	0.29	1.25	0.33
S	0.78	0.29	0.88	0.30
O	0.59	0.20	0.64	0.21
N	0.28	0.09	0.41	0.06

Table 4 Monthly mean values and the standard deviation (STD) taking all values (or the coincident) for the SP sites and the GNSS sites respectively.

Figure 3 shows clearly the differences between IWV_{GNSS} (red-diamond line) and IWV_{SP} (blue-dot-crosses line) values of the annual cycle where higher values for IWV_{GNSS} are observed during all the cycle. The minimal differences are observed on May, June and October confirming that the best agreement between GNSS and SP data are obtained for values in the middle of the measured IWV range, between 0.5 and 1.2 cm (0.5-1.7 for hourly data). In any case, the wider the range of IWV values, the better the photometer's performance is compared to GNSS data.

Although, as just mentioned, the differences between the data-bases, the annual cycle of IWV for RS taking the coincident data with SP was evaluated. As can be seen in Fig. 3, the IWV_{RS} (black-circle line) values present a very good agreement with those of SP (pink line) and fall between those of SP and GNSS, according to the expected results mentioned above. It must be noted the differences between the two data-bases used for SP during the months of September, October and November. These results highlighted the difficulties of these comparative analysis, but coincident data represent the real features over the behaviour of each instrument or technique.

5 Conclusions

This work focuses on the comparison of IWV values between GNSS and SP techniques in the Arctic area, based in our interest in analysing the capacity and behaviour of sun photometers by means of the availability of their IWV data in this complex

https://doi.org/10.5194/egusphere-2026-2374
Preprint. Discussion started: 20 May 2026

area. A total of 13 sites belonging to AERONET are available for this study covering a long period from 1997 at Barrow, but with very different periods for each site. On the other hand, the rapid expansion of the GNSS technique in the last 30 years has made possible a wide coverage over the world, and specially over the Arctic area, which facilitates the analysis of its data and the comparison with other techniques. 35 GNSS sites co-located with SP sites were available to compare with the 13 AERONET sites over all Arctic, where its vast extension and different characteristics can reflect the fact that averages values can be artificial numbers and that it is the values of each site that should really be considered.

Therefore, here a detailed analysis of the comparison of IWV from GNSS and SP is presented, taking coincident hourly data and with these results we try to obtain conclusions together with the results obtained in two previous works of Antuña-Marrero et al. (2022, 2025), where radiosonde and reanalysis were respectively compared with SP. The results clearly demonstrated the different behaviour of GNSS and SP depending on the values of IWV, where for values below 1.5 cm there is a prevalence of SP and when IWV increases that of GNSS. However, in general in the Arctic sites and spite of the low values of IWV in this area, the statistic parameters indicate a very good agreement between both techniques but with IWV_{GNSS} values higher than IWV_{SP}. The existent publications on the comparison of IWV in the Arctic demonstrated the dry bias of SP versus GNSS in agreement with our results.

The dry bias of SP behaviour was already detected in the comparison with radiosondes in Antuña-Marrero et al. (2022), where also a very good agreement in the comparison was reached. The low values of the statistical indicators in the two comparisons of GNSS-SP and RS-SP lead us to wonder if it is possible to conclude which of the three techniques presents the lowest (or highest) values, since there is not a direct GNSS-RS comparison. Although the different data-bases, for coincident hourly data we observed that the highest values of IWV are given by GNSS, radiosonde, SP and reanalysis in this order, with MBE (rMBE) in the range 0.02(7.5%)-0.06(1.9%) cm, according Tables 3-4 and Fig. 3 (reanalysis is not considered because is not based on a physical instrument).

The potential use of the AERONET sun photometers IWV observations for bias correction in the current ERA5 and MERRA-2 reanalyses has been raised. Those observations may also contribute to the assimilated datasets or to the quality control for the new MERRA-3 and ERA6 reanalyses.

https://doi.org/10.5194/egusphere-2026-2374
Preprint. Discussion started: 20 May 2026

Code and data availability

Integrated water vapor data from sun photometer from AERONET (2025) and from GNSS at Nevada Geodetic Laboratory website: https://geodesy.unr.edu

Author contributions

V. Cachorro: Writing and together with J. C. Antuña-Marrero: Original draft preparation, methodology, algorithms design and processing. A. Calle, D. Mateos, C. Toledano, J. C. Antuña-Sánchez, R. González, A. M. de Frutos Baraja: discussion. R. Román, M. Antón, J. Vaquero-Martínez: discussion and review. Javier Pacheco: preliminary processing.

Competing interests

The authors declare that they have no conflict of interest.

Acknowledgements

This work was supported by the Spanish "Ministerio de Ciencia e Innovación, MICINN", (Grants no. PID2021-127588OB-I00 and PID2024-157697OB-I00). This work was also funded by the European Commission through the EUBURN-RISK project (INTERREG-SUDOE; S2/2.4/F0327). The authors acknowledge the support of COST Action HARMONIA (CA21119) and the Spanish "Ministerio de Ciencia e Innovación, MICINN" to ACTRIS-ERIC. We acknowledge the support from the Laboratory of Disruptive Interdisciplinary Science (LADIS), at the University of Valladolid. J.C. Antuña-Marrero has been partially supported by the European 415 Metrology Program for Innovation and Research (EMPIR) within the joint research project 416 EMPIR 19ENV04 MAPP. The EMPIR is jointly funded by the EMPIR participating countries 417 within EURAMET and the European Union. Thanks are due to AERONET staff and PI sites for providing measurements and for the maintenance of the networks. GNSS IWV data was obtained from Nevada Geodetic Laboratory website: https://geodesy.unr.edu, where they are freely available, for which we are grateful.

Financial support

Ministerio de Ciencia e Innovación (MICINN), Grant no. PID2024-157697OB-I00. Project TED2021-131211B-I00375 funded by MCIN/AEI/10.13039/501100011033 and European Union, "NextGenerationEU"/PRTR. COST Action CA21119 HARMONIA. Department of Education, Junta de Castilla y León, and FEDER Funds, Reference: CLU-2023-1-05). European

https://doi.org/10.5194/egusphere-2026-2374
Preprint. Discussion started: 20 May 2026

Commission, EUBURN-RISK project (INTERREG-SUDOE; S2/2.4/F0327). Spanish Ministry for Science and Innovation to ACTRIS ERIC and the Marie Sklodowska-Curie Staff Exchange Actions Project GRASP-SYNERGY Grant no. 10 101131631.

References

AERONET. Integrated water vapor. AErosol RObotic NETwork. [Dataset] Retrieved from https://aeronet.gsfc.nasa.gov/new_web/index.html, 2025.

Antuña-Marrero, J. C., Román, R., Cachorro, V. E., Mateos, D., Toledano, C., Calle, A., Antuña-Sánchez, J. C., Vaquero-Martínez, J., Antón, M., and De Frutos Baraja, A. M.: Integrated water vapor over the Arctic: Comparison between radiosondes and sun photometer measurements, Atmospheric Research, 270, 1060XX-106059, https://doi.org/10.1016/j.atmosres.2022.106059, 2022.

Antuña-Marrero, J. C., Román, R., Cachorro, V. E., Mateos, D., Toledano, C., Calle, A., Antuña-Sánchez, J. C., Vaquero-Martínez, J., González, R., Antón, M., and De Frutos Baraja, A. M.: Comparing integrated water vapor sun photometer measurements over the Arctic with ERA5 and MERRA-2 reanalyses. Journal of Geophysical Research Atmospheres, 130, e2024JD041120. https://doi.org/10.1029/2024JD041120, 2025.

Barreto, A., Cuevas, E., Granados-Muñoz, M.J., Alados-Arboledas, L., Romero, P. M., Gröbner, J., Kouremeti, N., Almansa, A. F., Stone, T., and Toledano, C.: The new sun-sky-lunar Cimel CE318-T multiband photometer a comprehensive performance evaluation, Atmospheric Measurements. Techniques, 9, 631–654. https://doi:10.5194/amt-9-631-2016, 2016.

Bevis, M., Businger, S., Herring, T.A., Rocken, C., Anthes, R.A., Ware, R.H., GPS meteorology: Remote sensing of atmospheric water vapor using the global positioning system. J. Geophys. Res. 97, 15787. https://doi.org/10.1029/92JD01517, 1992.

Blewitt, G., Hammond, W. C., & Kreemer, C., Harnessing the GPS data explosion for interdisciplinary science. Eos, 99. https://doi.org/10.1029/2018EO104623, 2018.

Boehm, J., B.Werl, and H.Schuh, Troposphere mapping functions for GPS and very long baseline interferometry from European Centre for Medium-Range Weather Forecasts operational analysis data, J. Geophys. Res., 111, B02406, https://doi.org/10.1029/2005JB003629, 2006.

https://doi.org/10.5194/egusphere-2026-2374
Preprint. Discussion started: 20 May 2026

Campanelli, M., Mascitelli1, A., Sanò, P., Diémoz, H., Estellés, V., Federico, S.: Precipitable water vapor content from ESR/SKYNET sun–sky radiometers: validation against GNSS/GPS and AERONET over three different sites in Europe, Atmospheric Measurements Techniques, 11, 81–94, https://doi.org/10.5194/amt-11-81-2018, 2018.

Cubasch, U., Wuebbles, D., Chen, D., Facchini, M. C., Frame, D., Mahowald, N., and Winther, J. G.: Introduction. In Climate Change 2013: The Physical Science Basis. Contribution of Working Group I to the Fifth Assessment Report of the IPCC; Cambridge University Press: Cambridge, UK, https://www.ipcc.ch/site/assets/uploads/2017/09/WG1AR5_Chapter01_FINAL.pdf, 2013.

Davis, J.L., Herring, T.A., Shapiro, I.I., Rogers, A.E.E., Elgered, G., Geodesy by radio interferometry: Effects of atmospheric Modelling errors on estimates of baseline length. Radio Sci. 20, 1593–1607. https://doi.org/10.1029/RS020i006p01593, 1985.

Deryng, D., P. Poli, C. Buontempo, S. Burgess, C. Cagnazzo, H. Hersbach, A. Obregon and S. Vermoote, ERA6 User Community Neepp. 14,ds Position Paper (Version 2.0). ECMWF, Copernicus Climate Change Service (C3S). https://climate.copernicus.eu/sites/default/files/2024-04/ERA6%20Users%20Workshop%20Position%20Paper%20ECMWF%20v2%20240410.pdf, 2024.

Douville, H., Raghavan, K., Renwick, J., Allan, R.P., Arias, A. P., Barlow, M., Cerezo-Mota, R., Cherchi, A., Gan, T. Y., Gergis, J., Jiang, D., Khan, A., Pokam Mba, W., Rosenfeld, D., Tierney, J., and Zolina, O.: Water Cycle Changes. In Climate Change 2021: The Physical Science Basis. Contribution of Working Group I to the Sixth Assessment Report of the Intergovernmental Panel on Climate Change [Masson-Delmotte, V., P. Zhai, A. Pirani, S.L. Connors, C. Péan, S. Berger, N. Caud, Y. Chen, L. Goldfarb, M.I. Gomis, M. Huang, K. Leitzell, E. Lonnoy, J.B.R. Matthews, T.K. Maycock, T. Waterfield, O. Yelekçi, R. Yu, and B. Zhou (eds.)]. Cambridge University Press, Cambridge, United Kingdom and New York, NY, USA, pp. 1055–1210, https://doi.org/10.1017/9781009157896.010, 2021.

El Akkraoui, A., et al., Reanalysis activities at the NASA Global Modelling and Assimilation Office. NASA Technical Reports Server (NTRS). ID: 20230013282. https://ntrs.nasa.gov/api/citations/20230013282/downloads/ecmwf-as2023-elakkraoui.pdf, 2023.

García, R. D., Cuevas, E., Cachorro, V. E., García, O. E. , Barreto, A. , Almansa, A. F., Romero-Campos, P. M., Ramos, R., Pó, M., Hoogendijk, K., and Gross, J.: Water Vapor Retrievals from Spectral Direct Irradiance Measured with an EKO MS-711 Spectroradiometer—Intercomparison with Other Techniques, Remote Sensing, 13, 350, https://doi.org/10.3390/rs13030350, 2021.

Giles, D. M., Sinyuk, A., Sorokin, M. G., Schafer, J. S., Smirnov, A., Slutsker, I., et al.: Advancements in the Aerosol Robotic Network (AERONET) Version 3 database – Automated near-real-time quality control algorithm with improved cloud screening for Sun photometer aerosol optical depth (AOD) measurements. Atmospheric Measurement Techniques, 12(1), 169–209. https://doi.org/10.5194/amt-12-169-2019, 2019.

Gupta, P. and A. Sayeed, MERRA2_CNN_HAQAST_PM25: Hourly Bias-Corrected PM2.5 Datasets for Global Air Quality Assessment, Geoscience Data Journal, 13, 2, e70070, https://doi.org/10.1002/gdj3.70070, 2026.

https://doi.org/10.5194/egusphere-2026-2374
Preprint. Discussion started: 20 May 2026

Holben, B. N., Eck, T. F., Slutsker, I., Tanre, D., Buis, J. P., Setzer, A., et al., Aeronet – a federated instrument network and data archive for aerosol characterization. Remote Sensing of Environment, 66, 1–16. https://doi.org/10.1016/S0034-4257(98)00031-5, 1998.

Kruczyk, M.: Comparison of techniques for Integrated Precipitable Water measurement in the polar region, Geoinformation Issues, 7(1), 15–27, https://doi.org/10.34867/gi.2015.2, 2015.

Miloshevich, L. M. Vömel, H., Whiteman, D. N., Lesht, B. M., Schmidlin, F. J., and Russo, F.: Absolute accuracy of water vapor measurements from six operational radiosonde types launched during AWEX-G and implications for AIRS validation. Journal of Geophysical Research Atmospheres, 111, D09S10, https://doi.org/10.1029/2005JD006083, 2006.

Negusini, M., Petkov, B. H., Tornatore, V., Barindelli, S., Martelli, L., Sarti, P., & Tomasi, C.: Water vapour assessment using GNSS and radiosondes over polar regions and estimation of climatological trends from long-term time series analysis. Remote Sensing, 13(23), 4871, https://doi.org/10.3390/rs13234871, 2021.

Nygård, T., Naakka, T., and Vihma, T.: Horizontal Moisture Transport Dominates the Regional Moistening Patterns in the Arctic. Journal of Climate, 33(16), 6793–6807, https://doi.org/10.1175/jcli-d-19-0891.1, 2020.

Pérez-Ramírez, D., D. N. Whiteman, A. Smirnov, H. Lyamani, B. N. Holben, R. Pinker, M. Andrade, and L. Alados-Arboledas: Evaluation of AERONET precipitable water vapor versus microwave radiometry, GPS, and radiosondes at ARM sites, J. Geophys. Res. Atmos., 119, 9596–9613, https://doi.org/10.1002/2014JD021730, 2014.

Rinke, A., Segger, B., Crewell, S., Maturilli, M., Naakka, T., Nygård, T., Vihma, T., Alshawaf, F., Dick, G., Wickert, J., and Keller, J.: Trends of vertically integrated water vapor over the Arctic during 1979–2016: Consistent moistening all over? , Journal of Climate, 32(18), 6097–6116, https://doi.org/10.1175/jcli-d-19-0092.1, 2019

Schneider, M., Romero, P. M., Hase, F., Blumenstock, T., Cuevas, E., and Ramos, R.: Continuous quality assessment of atmospheric water vapor measurement techniques: FTIR, Cimel, MFRSR, GNSS, and Vaisala RS92. Atmos. Meas. Tech. 3, 323–338. https://doi.org/10.5194/amt-3-323-2010, 2010.

Smirnov, A., Holben, B. N., Lyapustin, A., Slutsker, I., and Eck, T. F.: AERONET processing algorithms refinement, AERONET2004 workshop, El Arenosillo, Spain, 10– 14 May 2004. https://aeronet.gsfc.nasa.gov/new_web/spain2004/presentations/Smirnov_Algorithm.ppt, 2004

Trenberth, K. E., and Stepaniak, D. P.: The flow of energy through the earth's climate system. Q. J. R. Meteorol. Soc., 130, 2677–2701, https://doi.org/10.1256/qj.04.83, 2004.

Van Malderen, R., Brenot, H., Pottiaux, E., Beirle, S., Hermans, C., De Maziere, M., et al: A multi-site intercomparison of integrated water vapour observations for climate change analysis. Atmospheric Measurement Techniques, 7(8), 2487–2512. https://doi.org/10.5194/amt-7-2487-2014, 2014.

Vaquero-Martínez, J., and M. Antón, Review on the role of GNSS Meteorology in monitoring water vapor for atmospheric physics. Remote Sens., 12, 2287, https://doi.org/10.3390/rs13122287, 2021.

https://doi.org/10.5194/egusphere-2026-2374
Preprint. Discussion started: 20 May 2026

Vaquero-Martínez, J., Bagorrilha, A. F., Antón, M., Antuña-Marrero, J. C., & Cachorro, V. E.: Comparison of CIMEL sun-photometer and ground-based GNSS integrated water vapor over south-western European sites. Atmospheric Research, 275, 106217, https://doi.org/10.1016/j.atmosres.2022.106217 , 2022.

Vihma, T., Screen, J., Tjernström, M., Newton, B., Zhang, X., Popova, V., Deser, C., Holland, M., and Prowse, T.: The atmospheric role in the Arctic water cycle: A review on processes, past and future changes, and their impacts. Journal of Geophysical Research: Biogeosciences, 121(3), 586–620, https://doi.org/10.1002/2015jg003132, 2016

Weaver, D., Strong, K., Schneider, M., Rowe, P. M., Sioris, C., Walker, K. A., Mariani, Z., Uttal, T., McElroy, C. T., Vömel, H., Spassiani, A., and Drummond, J. R.: Intercomparison of atmospheric water vapor measurements at a Canadian High Arctic site, Atmospheric Measurements Techniques. 10, 2851–2880, https://doi.org/10.5194/amt-10-2851-2017, 2017.

Zhang, Y., Cai, C., Chen, B., and Dai, W.: Consistency evaluation of precipitable water vapor derived from ERA5, ERA-Interim, GNSS, and radiosondes over China, Radio Science 54(7), 561-571, https://doi.org/10.1029/2018RS006789, 2019.

Weaver, D., Strong, K., Schneider, M., Rowe, P.M., Sioris, C., Walker, K.A., Mariani, Z., Uttal, T., McElroy, C.T., Vömel, H., Spassiani, A., Drummond, J.R.: Intercomparison of atmospheric water vapour measurements at a Canadian High Arctic site. Atmos. Meas. Tech. 10, 2851–2880., https://doi.org/10.5194/amt-10-2851-2017, 2017.

Wei, C., Zhao, X., Liu, Y., Yang, P., Zhou,Z., & Chen, Y., Bias analysis and correction of ERA5 reanalysis in the context of tropical cyclones. Journal of Geophysical Research: Atmospheres, 130, e2024JD042737. https://doi.org/10.1029/2024JD042737, 2025